

GODDARD
GRANT
JN-76-32
198636
548

Second Semi-Annual Progress Report

Submitted to NASA
for Grant# NAG5-1017 to Howard University

Title

Evaluation, Development, and Characterization of
Superconducting Materials for Space Application

Dr. A. N. Thorpe
Principal Investigator
Howard University

Dr. S. Alterescu
Technical Monitor
NASA Goddard

January 1989

(NASA-CR-184842) EVALUATION, DEVELOPMENT,
AND CHARACTERIZATION OF SUPERCONDUCTING
MATERIALS FOR SPACE APPLICATION Semiannual
Progress Report No. 2 (Howard Univ.) 54 p

N89-23302

CSCL 20L G3/76 0198636

Unclas

I. INTRODUCTION

The low magnetic field ($H < 100$ Oe.) properties of the high transition temperature superconducting copper oxides continues to be of fundamental¹ and technological² interest. Current fundamental interests are concerned with the consequences of treating bulk specimens as inhomogeneous, granular materials composed of superconducting (SC) regions, i.e. grains, clusters of grains, etc., imbedded in a nonsuperconducting host material. One postulates that in sintered samples the superconducting grains are electrically and magnetically coupled and, at a temperature T_{cc} less than the superconducting transition temperature, T_{cg} , of the grains, this coupling leads to phase-locking of the grains so as to render the entire sample superconducting³. Here one speaks of "fully" SC from the viewpoint that macroscopic supercurrents can flow so as to effectively shield the macroscopic volume of the sample from changes in an externally applied magnetic field i.e. "perfect" ac shielding. Observation of a reversible magnetization curve^{4,5} and of a specific heat jump⁶ at $T_c(H)$ when the sample is cooled in the presence of a magnetic field have been taken as independent evidence that in these high T_c oxides the superconducting grains per se are exhibiting a Meissner-Oschenfeld effect⁷. Finnemore et. al.⁴ showed that the detailed behavior of the magnetization curve could be explained if one treated their sintered sample as a collection of uncoupled spherical SC grains with dimensions of the order of the zero temperature superconducting penetration depth, $\lambda(0)$. Thus one arrives at a model in which intergranular supercurrents are responsible for the perfect ac shielding properties and supercurrents flowing on the surface of the grains give rise to the Meissner effect in the grains per se. Since macroscopic supercurrents must involve intergranular current flow, the low values of the

critical current density, J_c , in bulk samples and the breakdown of "perfect" ac shielding at low values of the ac magnetic field, h^{ac} , are viewed as being indicative of weak intergranular coupling^{1,2}. Two mechanisms have been singled out as possible sources of this weak coupling¹; Josephson tunneling if the nonsuperconducting (NSC) host is an insulator or semiconductor and proximity effect coupling if the NSC host is metallic. These coupling mechanisms which, if operative, govern the low magnetic field properties of bulk samples will be dominated by the nature, and width, of the grain boundaries present in the bulk material. In addition to these two effects one should also allow for the possibility that the intergranular material is a superconductor in its own right with somewhat reduced values for T_c and J_c .

The granular model is qualitatively consistent with the temperature induced magnetic moment observed when the sample is cooled in the presence of an externally applied dc magnetic field, H , the so-called field cooled (FC) scenario and the temperature dependence of the magnetic moment which results when a dc magnetic field, H , is applied to the sample after the sample had been cooled to $T \ll T_{cg}$ in zero applied field; the so-called zero-field cooled (ZFC) scenario⁸. For small, $\leq 10^2$ Oe., dc magnetic fields, the ZFC and FC data show a temperature region of near coincidence for T less than, but close to T_{cg} , i.e. $t = T/T_{cg} \geq 0.95$; thus one again invokes the picture of grains which show the Meissner effect and intergranular shielding currents which give rise to the observed trapping of magnetic flux.

There are, however, data which are in apparent conflict with the above model. Ginley et.al⁹ interpret results of their studies of the effect of pressure on the magnetic properties of sintered samples as strong evidence for superconducting regions comprised of a thin superconducting shell surrounding a normal metal core. If this is so then the Meissner effect can

not occur. Gracia et. al.¹⁰ interpret their ac magnetic susceptibility data as evidence that the superconducting regions are comprised of semiconducting and metallic regions with superconductivity being restricted to the semiconducting-metallic interfaces. These models conflict with that proposed by Finnemore et.al.⁴; a model subsequently used by Farrell et al.¹¹ to explain low field, dc magnetic susceptibility data obtained on sintered samples of YBCO. Thus while the granular model of these high T_c oxides is generally accepted there are conflicting data with regard to the nature and physical makeup of the SC grains (clusters) per se. as well as the effect of the intergranular phases.

As part of a program to fabricate high T_c thick films (thickness $\gg \lambda$) with enhanced $J_c(77\text{ K})$ values, we have investigated "bulk" samples prepared by different processing routes in order to enhance J_c values of the powders to be used in the thick film fabrication. One way to change the composition and physical distribution of the intergranular material, hence the intergranular coupling, is high temperature processing ($T \approx 1050\text{ }^\circ\text{C}$) of sintered material. Partial melting occurs at this temperature and the subsequent recrystallization from the melt produces clusters of large sized rectangular grains separated by a second phase material¹². We have used this route to produce samples of significantly different microstructures with similar T_c values but different low magnetic field properties.

We report here results of our low magnetic field studies of dc magnetic susceptibility and ac magnetic susceptibility ($\chi^{ac} = \chi' - i\chi''$) of bulk samples and powders. These data are analyzed and compared with the microstructures and compositions of the samples as determined by SEM micrographs, X-ray and chemical analysis. Particular emphasis is given to the interpretation of the χ^{ac} data which have been obtained as function of:

(a) the magnitude and frequency of the ac measuring field, $|h^{ac}|$ and (b) low values of an applied dc magnetic field, $H \leq 220$ Oe.

II. EXPERIMENTAL DETAILS

A. Sample characterization

Samples were prepared and characterized according to the procedures described in earlier publications^{12,13}. Briefly stated re-calcined powders were used to prepare pellets, 11 mm in diameter and 2-5 mm thick, by cold pressing, for use in the preparation of the sintered and recrystallized samples. The pellets were placed on alumina substrates inside a quartz liner in a tube furnace. The system was thoroughly flushed with oxygen and was held in oxygen under atmospheric pressure during the heat treatment of the pellets. The peak firing temperature was 990 °C for the sintered specimens and 1050 °C for the partially melted ones. In this paper we report data obtained on pellets prepared from the same master powder which were then fragmented to yield a variety of samples for the different studies carried out. In some cases the ac susceptibility data and dc magnetization studies were performed sequentially on the identical sample.

Differential thermal analysis data¹² show that no melting occurs at 990 °C while approximately 80% of the sample is melted at 1050 °C. Chemical analyses indicated that the relative molar concentrations of Y, Ba and Cu in end products of both heat treatments were 1:2:3. Oxygen content determinations yielded values of $x = (6.91 \pm 0.02)$ based on the formula $YBa_2Cu_3O_x$. The material prepared at 990 °C had a density, ρ , of (5.26 ± 0.03) g/cm³ while the 1050 °C material had $\rho = (6.32 \pm 0.03)$ g/cm³. Microstructural studies were performed using an Amray Model 1000A scanning electron microscope. X-ray diffraction patterns were obtained by use of a Siemens

D500 diffractometer over the range of 2θ values of 1° and 60° .

B. DC Magnetic Measurements

DC magnetic susceptibility studies were carried out by use of a Faraday balance¹⁴. Samples of approximately 90 mg were placed on the balance and cooled to 77 K with no current in the magnet. Susceptibility measurements were performed as the temperature of the sample was increased in temperature intervals of approximately 1K in a constant magnetic field. The temperature was measured using a FeAu-chromel thermocouple placed within a mm of the sample. A PARC vibrating coil magnetometer was used to obtain magnetization curves at 77 K. For these measurements the samples were in the form of a rectangular parallelopipeds measuring approximately $2.5 \times 3 \times 6 \text{ mm}^3$. Samples were cooled to 77 K in zero field and the measurements were initiated with with an applied field of 2.5 kOe. Data were obtained as the field was decreased in increments of about 10 Oe. After each field increment, measurements were taken after a time sufficient to allow flux drift to disappear. For the sintered sample the relaxation time was 1 minute while that of the remelted samples was 2.5 minutes.

C. AC Susceptibility Measurements

A modified Hartshorn type ac mutual inductance bridge¹⁵, was used to measure the complex mutual inductance, $M - M' - iM''$ of a copper coil system wound on a bakelite coil form. This coil system, consisting of a pair of oppositely wound secondaries and a common concentric primary winding or coil, was positioned around a glass vacuum chamber and the assembly was immersed in a constant temperature bath of liquid nitrogen. The overall

cryostat is a general purpose one used in the screening of new materials. A room temperature "loader" is used to position the sample in the center of one of the secondary coils with the coils at a constant temperature which for most of this study was 77 K. Although the coupling between sample and mutual inductance coils was not optimized, modern day amplifiers have sufficient gain so that one can obtain meaningful data without optimization of the coupling. The bridge was balanced with the coils empty and rebalanced with the sample positioned within one of the secondary coils. A two phase lock-in amplifier was used to monitor simultaneously, the voltage imbalances of the resistive (V_R) and reactive (V_Q) components of the bridge caused by the sample undergoing its normal (N) to superconducting (S) state transition. In a few cases the bridge was balanced with the sample in the S state and data were taken as the sample was heated through its SN transition. The phase of the two-phase amplifier was adjusted so that $V_Q(T) \approx \Delta M'(T)$ and $V_R(T) \approx \Delta M''(T)$. A carbon glass thermometer and a copper coil were simultaneously used as temperature sensing elements. A DMM was used to measure the resistance of the Cu coil.

Using V_Q and V_R to drive the Y-axes of the two pen recorder and the output of the DMM to drive the X axis one obtains simultaneous traces of $\Delta M'(T) \approx \Delta \chi_0'(T)$ and $\Delta M''(T) \approx \Delta \chi_0''(T)$ as functions of the temperature. Here $\chi_0^{ac}(T) = \chi_0'(T) - i\chi_0''(T)$ is the zero field complex ac magnetic susceptibility of the sample. Balancing the bridge with the sample in the normally conducting state results in $\Delta \chi_0'(T) = \chi_0'(N) - \chi_0'(T)$ and $\Delta \chi_0''(T) = \chi_0''(N) - \chi_0''(T)$. A liquid nitrogen cooled solenoid was used to provide small ($H \leq 220$ Oe) dc magnetic fields parallel to the ac measuring field, h^{ac} , when the differential magnetic susceptibility $\chi_H^{ac}(T) = \chi_H'(T) - i\chi_H''(T)$ was the parameter of interest.

Most of our data were obtained by the temperature sweep method in which one balances the bridge with no sample present, inserts the sample via a room temperature "loader" and rebalances the bridge with the temperature of the sample slightly below room temperature, and the bridge imbalances monitored as the sample slowly cools, in vacuum to 77 K. The sample is then displaced about 25 cm from the center of the coil, heated to about 130 K and reinserted into the coil. With a vacuum of $\approx 10^{-5}$ torr the cooling traces are reproducible to ± 0.05 K. This is very time consuming and since the object is a comparative study of many different samples, we usually adjusted the vacuum so that the sample cooled from 125 K to 78 K in about 2.5 to 3 hours. Under these conditions we found that our temperature reproducibility deteriorated and that we had a temperature uncertainty of ± 0.2 K. A value deemed adequate for our comparative studies. Implicit to the temperature sweep method is the fact that one can adjust the bridge so the $V_R(T)$ trace is not affected by the reactive imbalance reflected by the $V_Q(T)$ trace. For the oxides one has relatively small values for $V_R(T)$ so that the phase independence of the two imbalances is of concern. We verified that the qualitative behaviors of the two traces were independent by performing a point by point determination of $\Delta M'(T)$ and $\Delta M''(T)$. Here one employs a heater to hold T at a constant value and the bridge is balanced. The temperature is changed to a new constant value and the bridge rebalance, etc. Plots of the resulting $M'(T)$ and $M''(T)$ versus temperature were qualitatively the same as the $V_Q(T)$ and $V_R(T)$ traces. Nevertheless before each sweep extra care was taken with the phase adjustment to minimize "phase-mixing" of the $V_Q(T)$ and $V_R(T)$. Purity of the two imbalances was always verified after each NS transition had occurred.

III. RESULTS

Scanning Electron Micrographs (SEM), typical of samples prepared by sintering and recrystallization-from-the-melt are presented in Fig.1a and 1b respectively. The microstructure of the sintered sample is typical of these high T_c oxides being composed of irregularly-shaped, radomly-oriented grains with dimensions in the 5 to 20 μm range. We estimate a void volume of about 10%. The microstructre of the partially melted sample is composed of grains well aligned in the a-b plane, typically 20 μm wide and 100 μm long, with minimal grain boundary disruption. Twinning was extensive. A small amount ($\approx 10\%$) of an amorphous like phase is evident. Relatively few voids are noted when compared with the microstructure of sintered samples.

In the course of our study, dc magnetization curves have been measured for a variety of samples at field values between ± 0.25 T. In general the sintered samples display the least amount of hysteresis and data typical of this class of samples are presented in Fig.2a. All samples prepared from the melt show increased hysteresis over that of the sintered samples with the largest amount, Fig.2b, being observed for the sample with the microstructure shown in Fig.1b. Whereas the amount of hysteresis exhibited by the melted sample is remakably large for $T=77$ K, the relatively small amount of hysteresis exhibited by the sintered sample is consistent with published reports¹⁶. DC magnetic susceptibilty as a function of temperature, T , for three values of the applied dc magnetic field are shown in Fig. 3.

Traditionally ac susceptibility techniques used in the search for, and study of, new superconductors emphasize low frequencies ($f < 100$ Hz) and low ac magnetic fields ($|h^{ac}| < 0.1$ Oe.). Low frequencies minimize effects of eddy currents in the addendum and low ac fields are in keeping with the definition of χ_0^{ac} . While we have concentrated on measurements for

$|h^{ac}| < 1.2$ Oe. we have on a few occasions used higher $|h^{ac}|$ values. In Fig. 4 we present XY recorder traces of $V_Q(T) \approx f|h^{ac}|\Delta M'(T) \approx \Delta\chi_0'(T)$ and $V_R(T) \approx f|h^{ac}|\Delta M''(T) \approx \Delta\chi_0''(T)$ for samples whose magnetization curves are presented in Fig. 2. Data are shown for several values of $|h^{ac}|$ at fixed values of f . In these Figs. we have normalized the $V_Q(T)$ to an $|h^{ac}|$ of 1.5 Oe and denote this quantity by $V_Q^*(T)$.

The effects of small (≤ 250 Oe) superimposed dc magnetic fields, H , on the $V_Q(T)$ and $V_R(T)$ traces for the sintered and melted samples are shown in Figs. 5. For these measurements H was parallel to h^{ac} and was applied with the sample in the normal state. In this situation $V_Q(T) \approx \Delta\chi_H'(T)$ and $V_R(T) \approx \Delta\chi_H''(T)$, see Sec. II.C.

After the above data were obtained a portion of the pellet of microstructure 1b was rendered into the form of a powder, average grain size ≈ 1 microns. The resulting magnetization curve showed that powdering the sample produced a decrease in magnetic hysteresis approaching that observed for the sintered sample. Approximately 0.18 gms. of this fine powder was placed in a capsule containing slightly warmed apieazon N grease, stirred and allowed to settle. Results of our χ_0^{ac} measurements are presented in Fig 6. Data obtained with a larger quantity of a more coarse powder obtained from the same master melt are also shown in Fig. 6.

IV. DISCUSSION

A. DC Magnetization Data

Data in Fig. 2 indicate that the maximum diamagnetic moment is attained for values of H in the 90 to 120 Oe range. Qualitatively speaking such magnetization curves are typical of hysteretic type II superconductors. Experimentally one defines strong versus weak flux pinning in a

superconductor by the magnitude of the change in magnetic moment, δM , which accompanies a small decrease, δH , in the applied dc magnetic field. If the sample traps all the magnetic flux associated with the δH , the slope of the return curve should be equal to the initial slope of the virgin magnetization curve. Based on this δM criterion, data of Figs. 2a, & b clearly indicate that the microstructure of the "recrystallized-from-the-melt" samples exhibit enhanced flux pinning over that of the sintered sample. The amount of magnetic hysteresis in Fig. 2b, is comparable to that which, until now, has only been seen at much lower temperatures¹⁷.

Early studies by Schweitzer and Bertman¹⁸ showed that hollow and solid cylinders of low κ type II superconductors yielded essentially the same magnetization data and concluded that the observed hysteresis was due to surface currents. In the case of high κ materials in which bulk hysteresis, or pinning, dominates surface effects, Fietz and Webb¹⁹ showed the $J_c(H,T) \approx \Delta M(+,-)$ where $\Delta M(+,-)$ is the difference between the magnetic moment, M , at a given value of the applied dc magnetic field, H , measured with H increasing and decreasing in value. For high κ materials the critical state concept²⁰ describes a current distribution throughout the superconductor that is determined by the effectiveness of material inhomogeneities in pinning a flux distribution against the action of Lorentz-type forces. Use of the critical state model allows one to evaluate the constant of proportionality between J_c and $\Delta M(+,-)$. Straightforward application of the above procedure to evaluate $J_c(H,T)$ for bulk samples of the high T_c oxides, results²¹ in a $J_c(2.3 \text{ K}, 5 \text{ kOe})$ of 10^5 A/cm^2 falling rapidly with increasing temperatures to $\approx 10^2 \text{ A/cm}^2$ at 77 K. This lower value is consistent with values of $J_c(0, 77 \text{ K})$ obtained via transport current measurements.

There is no feature in the magnetization data of Fig 2 that suggests

one is dealing with a granular material. However the reversibility of the high field ($H > 5T$) portion of the magnetization curves of these high T_c oxides led Finnemore et al⁴, to associate the higher field values of M with supercurrents flowing on the surfaces of the individual grains and not with intergranular or intercluster shielding currents. In this context it should be noted that the near reversibility of the high magnetic field portion of the magnetization curves^{4,5} and an increase in hysteresis at lower temperatures are also observed with nongranular high field superconducting alloys²². However, successes¹¹ of the independent grain model has led to the use of the grain size, and not the macroscopic dimensions of the sample, in applying the technique of Feitz and Webb¹⁹ to an analysis of high field magnetization data. In keeping with this practice, and assuming the data of Fig. 2 is applicable to a system of decoupled spherical grains of ≈ 2 microns, results in the $J_c(H, 77 K)$ values shown in the insert of Figs. 2a,b. Based on this analysis, the resulting order of magnitude increase in J_c for the recrystallized sample implies the presence of enhanced pinning sites within the grains. The preceding analysis ignores the presence of the second phase in the recrystallized sample as it deals only with shielding currents associated with the individual grains. A decrease in magnetic hysteresis and the absence of a peak in $V_p(T)$ observed upon rendering the sample into the form of a fine powder, Fig. 6, suggests that the role of the second phase may not be a passive one as far as the magnetization data is concerned. Since the second phase is located in the intergranular regions it is logical that it affects only the intergranular currents causing one to question the validity, for the field values employed, of the above analysis based solely on intragranular shielding currents.

DC susceptibility data, Fig. 3, show that χ^{dc} is still temperature

dependent at 77 K for fields as low as 220 Oe. This is an expected result since magnetization data indicate that $220 \text{ Oe.} > H_{c1}(77 \text{ K})$. Therefore the samples are still in their mixed state where χ^{dc} is temperature dependent. Since magnetization data alone can not pinpoint the nature of the pinning sites operative in the mixed state, it was felt that a study of the ac magnetic susceptibility in conjunction with magnetization data might shed additional light on the nature of this pinning²³.

B. AC magnetic susceptibility.

1. Background

The advent of high T_c oxides has produced a significant increase in the use of ac induction techniques to investigate the superconducting transitions of these complex metallurgical materials. It is not uncommon to read that a $\Delta\chi_0''(T)$ response of the kind seen in Fig. 4b,d,f for $|h^{ac}| \approx 10^{-1} \text{ Oe.}$ is typical of a normal to superconducting state (NS) transition and that structure in the $V_R(T) \approx \Delta\chi_0''(T)$ trace can be used to obtain information about the intra- and intergranular processes²⁴ as well as the energy gap²⁵. Since the granular nature of the high T_c oxides is central to current theoretical models of these materials^{1,2}, we feel a detailed discussion of the basis for interpreting χ^{ac} data is warranted.

What determines the χ^{ac} signature of a SC transition? Lauer mann and Shoenberg's²⁶ early use of a Hartshorn bridge to measure the in-phase and out-of phase components of the complex mutual inductance, $M = M' - iM''$, of a pair of secondary coils, with the sample positioned at the center of one of the secondary coils, showed that the signature of a NS transition is that both $\Delta M'(T)$ and $\Delta M''(T)$ are monotonically decreasing functions of the temperature. This fact has been substantiated in numerous studies over the

past fifty years and an example of this behavior is included in Fig. 10. Magnetic responses such as those in Figs. 4b,d,f & 5 are typical of hysteretic superconductors. Since these responses reflect the "perfect ac shielding" aspects of the $R_{dc} = 0$ state, $V_Q(T)$ should become strongly diamagnetic only at temperatures below that of the $R_{dc} = 0$ transition; i.e. only after macroscopic shielding currents can flow on the "surface" of the the sample. That this is indeed the case for the YBCO is clearly evident from simultaneous measurements of R_{dc} and χ_0^{ac} as functions of the temperature, see Fig.7. Clearly while the magnetic transition is initiated close to the start of the resistive transition, the bulk of the magnetic transition takes place only, after the $R_{dc} = 0$ state has been attained:

Comparison of data in Fig. 4 with that for a dilute, homogeneous alloy such as $TiCr_{1.65}$, shown in Fig.8, supports our contention that the present data are typical of a hysteretic SC alloy or element. Khoder²⁷ is of a different opinion. He presents a theoretical argument which requires that a peak in $\Delta\chi_0''(T)$ must occur at $T \approx T_{c0}$ even in the case of an ideal material showing the Meissner-Ochsenfeld effect. A small peak in the $\Delta\chi_0''(T)$ data for Sn at 5000 Hz reported by Couach et. al.²⁸ is viewed as evidence in support of this theory which has been recently applied to granular systems²⁹. Thus the significance of a peak in $\chi_0''(T)$ is still a matter of controversy, see section IV.B.3.

The $V_Q(T)$ traces, Fig. 4a,c,d, indicate that the transition widths, particularly those of the sintered sample, are relatively sharp and considerably sharper than similar transitions observed in early studies of high T_c A15 compounds such as Nb_3Ge ³⁰. What factors determine the experimentally observed width of such magnetic transitions? T_{c0} is determined by the condition that $|h^{ac}| = H_c(T_{c0})$ or $H_{c2}(T_{c0})$ whereas T_{cc} is

determined by $|h^{ac}| = (1-N)H_c(T_{cc})$ or $(1-N)H_{c1}(T_{cc})$. The former condition applies to both ideal and nonideal, i.e. hysteretic, transitions while the latter is applicable only to ideally reversible transitions. These equations yield $T_{co} - T_{cc} = |h^{ac}|(N/1-N)/(dH_c/dT)T_{co}$ for a type I superconductor. If one takes $|h^{ac}| = 0.1$ Oe, $N=1/3$ and a slope of 100 Oe/K, the ideal width for a type I superconductor such as Sn one finds an ideal width ΔT_c of 5×10^{-4} K. Data for annealed Sn, in Fig 10a, show that small amounts of chemical or physical impurities can lead to observed widths far in excess of this ideal value. In the case of hysteretic samples, such as the machined cylinder of Nb, the width of the transition is governed by the detailed temperature dependence of the magnetic hysteresis loops associated with $|h^{ac}|$ and not with the slope of the magnetization curve per se.

Our expression for the transition width is based upon the correlation between $\chi_0'(T)$ and the temperature dependence of the quantity $[dM/dh]_{h \rightarrow 0}$ of a reversible magnetization curve for a Type I superconductor with demagnetization factor N . In this case the observed $\Delta V_Q(NS) \approx \Delta \chi_0'(NS) \approx -1/4\pi(1-N)$ provided $\chi_0'(N) \approx 0$. For a hysteretic superconductor $\chi_0'(T)$ is related to the temperature dependence of the effective slope of the hysteresis curves associated with h^{ac} and $\chi_0'(S)$ is governed by the perfect shielding aspect of the $R_{dc} = 0$ state. In this case the magnitude of the transition, i.e. $|\Delta \chi_0'(NS)|$ is not proportional to the superconducting volume but is proportional to the difference in the effectively shielded cross-sections or volumes of the N and S states. This difference can be orders of magnitude larger than the actual SC volume^{31,32}.

We have been discussing data obtained with $|h^{ac}|$ values of order 10^{-1} Oe. or less and have referred to such data as the zero field ac magnetic susceptibility denoted as χ_0^{ac} . A quantity sometimes referred to as the initial

susceptibility, i.e. the susceptibility one measures in the limit of vanishingly small measuring fields. In this context "small" is in relation to $H_{c1}(T)$ of the sample. In the case of a hysteretic superconductor one expects $\Delta V_Q(NS)$ to be linear in $|h^{ac}|$ as long as $\chi_0'(S)$ for the value of $|h^{ac}|$ being used approximates that of perfect ac magnetic shielding. Based on these considerations one can use $\chi_0'(T)$ data to obtain a quantitative measure of T_{c0} and ΔT_c but in general, the detailed shape of the $V_Q(T)$ traces yields only qualitative information about the purity and nature of the SC "phase" present in the sample. Thus the recent reemphasize on the simultaneous measurement of $\chi_0''(T)$ as a function of $|h^{ac}|$ in the belief that such data are capable of discerning inter- versus intragranular behavior.

The microstructure in Fig.1 is reminiscent of what Mendelssohn must have had in mind when he developed his superconducting sponge model³³ to explain irreversibilities in the magnetization curve of alloys. It has been postulated³⁴ that the granular microstructures of Fig.1 form, in effect, a special kind of Mendelssohn sponge involving "weak-links", see Sec.I. Due to the postulated "weak" nature of the proposed intergranular coupling one expects the magnitude of such lossless intergranular shielding currents, for a given T , to be significantly reduced by small increases in $|h^{ac}|$ or H . In this picture the "reversible" portion of the M vs T curves of the FC and ZFC scenarios as well as the reversible nature of the high field magnetization curve are attributed to the reversible magnetic properties of the SC grains per se. Although we believe that a peak in $\Delta\chi_0''(T)$ implies magnetic hysteresis, one can obtain more definitive information with regard to the thermodynamical reversibility of the magnetization curve through measurements of $\chi_H'(T)$ and $\chi_H''(T)$. A reversible magnetization curve requires the observation of a differential paramagnetic effect or DPE³⁵ in

the $\chi_H'(T)$ response. Thus measurements of χ_H^{ac} are an important complement to χ_0^{ac} data. With this background in mind we now turn to a discussion of our χ^{ac} data.

2. $\chi_0'(T)$ data

During the past year we have screened a large number of samples, but our discussion will center on only two samples which are representative of the two types of microstructures under investigation. Results obtained with these two specimens highlight problems associated with interpretations of $\chi^{ac}(T)$ measurements. Data in Fig. 3a-d show that the reactive imbalances, $V_Q(T) \approx \Delta\chi_0'(T) = |\chi_0'(N) - \chi_0'(T)|$, while indicating similar transition temperatures, i.e. T_c (onset) = $T_{co} = 90.4 \pm 0.2K$ for the sintered sample and $90.0 \pm 0.2K$ for the recrystallized samples, exhibit significant differences in their detailed behavior. These transitions are, with one notable exception, typical of superconducting alloys. The exception is the presence of an inflection point in the $V_Q(T)$ traces of the sintered sample which otherwise are relatively sharp yielding a $T_c(\text{completion}) - T_{cc} = 89.9 K$ for $|h^{ac}| \approx 10^{-1}$ Oe. This feature in the $V_Q(T)$ traces was also observed in sintered samples prepared at the U.S. Naval Research Laboratory, Fig. 7, but not in data obtained³⁸ with a Pb replica. The data for Pb ruled out geometrical effects as a cause for the inflection point and established that complete diamagnetic screening occurs in these high T_c sintered samples with $|h^{ac}| \approx 10^{-1}$ Oe. Whereas melted samples show a reasonably sharp initial decrease they exhibited an extended low temperature "tail". A feature which precludes a T_{cc} determination from the data of Fig. 3d. A check at lower temperatures showed that in general there is an additional 10% increase over the 77 K value in the diamagnetism of the melted samples which becomes essentially

temperature independent at $T \approx 55$ K. In keeping with current practice we note that if temperatures corresponding to $\Delta V_Q(T) = 0.1$ and 0.9 of $\Delta V_Q(NS)$ are used to define a transition width, ΔT_c , then the transition widths³⁶ for the melt grown samples are considerably broader than that of the sintered sample, e.g. 4 K and 1 K respectively for $|h^{ac}| \approx 10^{-1}$ Oe. For these high T_c oxides, reported values¹ of $(dH_{c2}/dT)_{T-T_c}$ are so large that, given the values of $|h^{ac}|$ used in this study, one would expect shifts in T_{c0} due to the increase in $|h^{ac}|$ to be too small to be observed. This would not be so if there were significant positive curvature of the critical field curve in the vicinity of T_{c0} . On the other hand $(dH_{c1}/dT)_{T-T_c}$ is stated to be ≈ 10 Oe/K and a decrease in T_{cc} should be observed. Traditionally the practice of quoting values for the midpoint of the transition, T_{cm} , arose from the need of an experimentally, well-defined fiducial point for use in comparing the magnetic behavior of SC alloys and compounds exhibiting broad, rounded transitions. For nonideal superconductors, T_{cm} has no fundamental significance of which the authors are aware. Clearly if T_{c0} is constant and T_{cc} decreases with increase in $|h^{ac}|$ a concomitant decrease in T_{cm} is to be expected.

The observed structure in $V_Q(T)$ for the sintered samples is characteristic of two superconducting transitions. In view of the granular models of these materials, one is tempted to interpret this inflection point as a manifestation of a change from intra- to intergranular shielding. However such structure can arise from other causes. For example structure in $V_Q(T)$ traces similar to that observed for the sintered sample was reported by Cox and Das³⁷ for a single phase sample of V_3Ga . Their sample although single-phase, i.e. the A15 phase, possessed a compositional gradient at its surface. For this A15 compound the compositional gradient results in a higher T_{c0} material being surrounded by a lower T_{c0} surface "layer". Such a

configuration of superconducting regions will give rise to structure in $V_Q(T)$ traces similar to that observed for the sintered sample. Lacking any direct evidence of a compositional gradient at the surfaces of our YBCO samples, we experimentally investigated this question by cutting the original 0.5" diameter pellet into several bar shaped specimens and reran the experiments. Aside from a decrease in the magnitude of the imbalanced voltages, due to decreased sample size, the data were indistinguishable from that obtained with the original pellet. Thus if the observed change in slope is due to a surface layer per se, this surface layer forms in a very short time after being exposed to ambient conditions. A more likely cause for this behavior is the presence of regions of slightly different T_{c0} values distributed more or less evenly throughout the sample.

The main effect of increasing $|h^{ac}|$ is a general broadening of the transition width as $|h^{ac}|$ is increased from 0.015 to 6.0 Oe. The shift the midpoint of the $V_Q(T)$ traces for the sintered sample, $\Delta T_{cm} = -4$ K for a $\delta|h^{ac}|$ of 6 Oe. appears to be a general property of sintered high T_c oxides as noted by earlier workers^{6,24,29,39,40}. This feature is not unique to high T_c sintered materials as the observed shifts in the midpoints of the $TiCr_{1.65}$ alloy, a low T_c material, is comparable in magnitude when expressed in terms of a reduced temperature, i.e. $\Delta T_c/T_c$, see Fig.8. The $V_Q(T)$ data of Fig. 4c were obtained after a six months interval from that of Fig. 4e. The sample was stored in air, and no significant qualitative difference in this ac response is obvious.

Additional noteworthy features in the data of Fig.4 are: (a) the inflection point in the $V_Q(T)$ traces of Fig.4a is displaced to lower temperatures and broadens into a plateau-like region with increase in $|h^{ac}|$, and, (b) although a strictly temperature independent value of $V_Q(T)$ is not

observed at the highest $|h^{ac}|$ values for $T = 77$ K, one sees that the increase in $\Delta V_Q(NS)$ for the sintered sample is linear in $|h^{ac}|$ to within 10%. This last observation allows one to state that $\Delta\chi_0''(NS)$ is essentially a constant over this range of ac measuring fields. A result at variance with those of Raboutou et al⁴¹. These investigators, using an inductive technique, reported a dependence of the total induced voltage V_{in} on $|h^{ac}|$. They found that at $T=77$ K, the quantity $V_{in}/|h^{ac}| \approx$ "effective" magnetic permeability is a constant, V_c , for $|h^{ac}| < 10^{-2}$ Oe and increases in value as h^{ac} increases taking on a new larger (a factor of three increase) constant value, V_s , for $h^{ac} > 7$ Oe. Since $V_{in} = (V_Q^2 + V_R^2)^{1/2} \approx V_Q$, if $V_Q \gg V_R$, one would expect, based on their results, to see the effects of this transition region in our V_Q data as well as in other published reports^{6,10,24,25,29,39,40}. If their data are typical of a collection of weakly coupled SC grains then our result that $\Delta V_Q(NS)/h^{ac} \approx$ constant would be evidence that the granular nature of our samples does not play an important role in determining the $V_Q(T)$ response. We have no explanation for this discrepancy.

3. $\chi_0''(T)$ Data

Setting $V_R(\text{peak}) - V_R(\text{normal}) = \Delta V_R(PN)$ and defining $\Delta V_R(PN)/\Delta V_R(NS)$ as a measure of the relative peak height, one notes, Fig.4a, that at the lowest $|h^{ac}|$ values the sintered sample exhibits a single, relatively large peak with a steep slope on its high temperature side and a gradual fall off on the low temperature side. Melted samples, Figs.4c,e, display smaller and more rounded peaks which exhibit a variety of substructures. A prominent features of the $V_R(T) \approx \Delta\chi_0''(T)$ traces of Fig.4 is the effect which increasing $|h^{ac}|$ has upon the detailed shapes of these traces and on the temperature at which the peak, or peaks, occurs.

Although it's been 25 years since Maxwell and Strongin⁴² drew attention to the existence of the "extra-loss" peak in $\chi_0''(T)$ data, a universally accepted interpretation of its significance is yet to be established. Regardless of its exact cause, the abrupt increase in $V_R(T) \approx \Delta\chi_0''(T)$, observed upon cooling the sintered sample(s) to $T < T_{c0}$ is a manifestation of the onset of increased ac losses in the mixed state of the sample as defined by the $V_Q(T)$ trace. Expansion of the data in the vicinity of T_{c0} shows that a small increase in $\Delta\chi_0''(T)$ does set in at $T = T_{c0}$ and that the abrupt rise occurs at a value of T slightly below that of the inflection point in $V_Q(T)$.

The gradual fall off of $V_R(T)$, on the low temperature side of the peak, Fig.4b, is similar to that observed with the TiCr alloy, Fig.8b, a nongranular superconductor where one accounts for the loss peak on the basis of either the eddy-current⁴² or magnetic hysteresis models⁴³, see Ref. 31 for a review of these models. In the case of granular superconductors, one also has to consider dissipative mechanisms due to the proposed network of superconducting loops containing Josephson junctions or weak-links. Ishida and Mazaki⁴⁴ developed a phenomenological model to account for dissipative effects in such a network and showed that the shape of the extra-loss peak depends on the type of "coupling" within in the superconducting network. For a tunnel junction one has a symmetric loss peak while a microbridge leads to an asymmetric peak. This model of Ishida and Mazaki⁴⁴ predicts that T_{c0} is independent of $|h^{ac}|$, and that both T_{cm} and T_p , the temperature of the peak, are shifted to lower temperatures with increase in $|h^{ac}|$. For a system of microbridges they find that $T_p \approx h^{2/3}$.

The data of Fig.4d for $|h^{ac}| < 2.2$, Oe can be fitted by $T_p(h) = (88.3 - 0.85h^{2/3})$ with the higher $|h^{ac}|$ data falling below an extension of this equation, see insert Fig.4d. Here T_p is in degrees K and h is in Oe. Thus one

could interpret this dependence as being indicative of microbridges being associated with intergranular shielding. It must be noted that nongranular alloys also show this negative displacement of T_p with increasing values of $|h^{ac}|$. For example the TiCr alloy of Fig. 8 with a T_{c0} of only 3.44 K exhibits an initial displacement of the peak which also follows an $h^{2/3}$ dependence. Based on this observation a negative shift in T_p at low $|h^{ac}|$ values which follows a $h^{2/3}$ dependence is not sufficient proof of intergranular superconductivity. There is however one very noteworthy difference in the behavior of the two materials. Data for the TiCr alloy show that the peak broadens with increasing $|h^{ac}|$ but that its shape remains invariant whereas structure becomes evident in the data for the sintered sample at the higher $|h^{ac}|$ values.

Comparing the two imbalanced voltages i.e. $V_Q(T)$ and $V_R(T)$ for the sintered sample, Figure 4a,b shows that as $|h^{ac}|$ is increased the main extra loss peak in $V_R(T)$ continues to be correlated with the inflection point in the $V_Q(T) \approx \Delta \chi_0'(T)$ traces and that a small, $\approx 1\%$ of $V_R(PN)$ secondary maximum emerges at $T \approx T_{c0}$. In an earlier study Goldfarb et al⁴⁵, reported a single, broad "extra-loss" peak with no corresponding signature in their $\chi_0'(T)$ data for values of $|h^{ac}| \leq 7$ Oe. In a subsequent report⁴⁰ structure in $\chi_0'(T)$ data, obtained with $|h^{ac}| = 1$ Oe. and higher, was found to be associated with two loss-peaks. A small one at $T \approx T_{c0}$ and a shifted main peak; data qualitatively similar to those in Fig.4b. Differences in the behavior of their two sets of samples were originally attributed⁴⁰ to the fact that the original samples had been subsequently annealed in oxygen. A procedure which presumably produced two distinct superconducting phases in the annealed specimens. In a note added in proof the role the oxygen in producing this effect was questioned. C. Ayache et al⁴⁶ have also reported the evolution of

two peaks with increasing $|h^{ac}|$. Their results for $|h^{ac}| = 0.01$ Oe are very similar to that shown in Fig. 4a,b with the exception that no inflection point is evident in the $\chi_0'(T)$ trace and $\chi_0''(S)$ is significantly larger than $\chi_0''(N)$. For $|h^{ac}| = 7.0$ Oe the original low field peak is practically undisturbed and a second, broad peak, of magnitude nearly equals that of the undisturbed peak, is observed centered at 82 K. This second peak is accompanied by an inflection point in the $\chi_0'(T)$ trace. Once again $\chi_0''(S) > \chi_0''(N)$. Garcia et al.¹⁰ present 1 kHz data obtained on a pressurized YBCO pellet. To temperatures as low as 10 K, only a single loss peak was observed for $h^{ac} = 0.1$ and 1 Oe and any peak in the 10 Oe data must lie at $T < 10$ K. They also find that $\chi_0''(T < T_{c0}) > \chi_0''(N)$. This result evident in some of our data as well as in other published reports is a disquieting one. We will return to a discussion of this point.

Renker et al.⁴⁷ present χ_0' and χ_0'' data on both a bulk sintered sample of a La-Sr-Cu-O compound and on powder obtained from the bulk sample. Data presented for a sintered sample show a single, broad extra-loss peak in $\chi_0''(T)$ and plots of $\chi_H''(T)$ obtained at $H = 5$ kOe show two loss peaks. These data were obtained with $f = 11$ Hz but $|h^{ac}|$ was not specified other than a statement to the effect that values between 0.1 and 10 Oe. had been used. They also observed a temperature dependent $\chi_0''(T < T_{c0}) > \chi_0''(N)$. Suprisingly the only effect of powdering was to broaden the peak and produce a smaller $\chi_0''(T < T_{c0})$, which, while still larger than $\chi_0''(N)$, was independent of the temperature for $T < 15$ K. This result led the authors to conclude that the peak in $\chi_0''(T)$ is due to loss-free shielding currents flowing on the surfaces of the isolated grains. If one has loss-free currents, what causes the peak?

Referring to their earlier results on sintered samples of YBCO which

show a small loss peak at $T = T_{co}$ and a larger second larger loss peak at $T < T_{co}$. Kupfer et al.⁴⁸ arrive at the opposite conclusion; i.e. when one observes a single extra-loss peak, the peak is due to intergranular SC. In addition they state that the observation of a single extra-loss peak is an indication that the sample was "not well prepared". We do not agree with such an assessment which conflicts with the present results and those of Goldfarb et al.^{40,45} and Ayache et al.⁴⁶ in that the number of peaks one observes is a function of $|h^{ac}|$.

The $V_R(T)$ responses for the melted samples, Figs. 4d & f, display quite different, and more complex, behavior from that of the sintered sample. In general only one extra-loss peak is observed, but the peak contains substructure which varies in detail from sample to sample and is a function of $|h^{ac}|$. However some general remarks can be made. The ratio of $\Delta V_R(PN)/\Delta V_Q(NS)$ for given values of $|h^{ac}|$ and f is about a factor of five smaller than that observed for the sintered sample and substructure is evident in the $f=17$ Hz data of Fig. 4f at the lower field values. As $|h^{ac}|$ is increased the higher temperature portion of the peak grows in relationship to the lower temperature portion so that at the highest value of $|h^{ac}|$ only a single broad peak is evident. Frequency effects have been ruled out as the data of Fig. 4d is essentially unchange at $f=34$, and 68 Hz. A check to helium temperatures, courtesy of the Naval Research Laboratory, indicated that for $|h^{ac}| = 0.6$ Oe. the peak seen in the data of Figure 4d is the only peak exhibited by this sample.

This perplexing array of $\Delta\chi_0''(T)$ responses caused us to question, whether the results are characteristic of the samples or due to some experimental artifact. Thus we simply interchanged the YBCO sample with similarly sized samples of Pb and Nb. Whereas the small, single extra-loss

peak in the Pb data was as expected for a slightly impure type I superconductor, the Nb results showed substructure in the loss peak, Fig.9b,c demonstrating the occurrence of double or multiple loss peaks is not unique to granular systems. The Nb data Fig.9 show the expected result that $\chi_0''(S) < \chi_0''(N)$ and that $\Delta\chi_0''(NS)$ increases with f in keeping with increased eddy-current losses in the normal state. In the past when such structure was observed in the loss peak of nongranular SC systems, it was attributed to the presence of two or more SC phases with slightly different values for T_c ; see Ref. 28 for an example of such substructure in a single crystal of V_3Si . For the case of a single component system, such as our machined cylinder of Nb, physical impurities can lead to the observation of multiple peaks in the $V_R(T)$ traces. Structure in the loss peak of Nb is not an edge effect as the structure persisted after the sharp edges of the sample had been rounded. From these results one can only conclude that interpretations of substructure in the extra-loss peak as being due to intra-and intergranular SC may be premature. The role of surface inhomogeneities in determining the ac responses of these high T_c oxides must be ascertained before one can justify such a detailed analysis.

A traditional means of eliminating the shielding effects of a SC network, due to a minority phase, in measurements of χ^{ac} is to render the bulk sample into the form of a fine powder and repeat the measurements. For the high T_c oxides one has conflicting results. Two extreme cases are found in the reports of Renker et al⁴⁷ Alpfenstedt et al⁴⁹. The former report shows that the effect of powdering the sample is to simply broaden the peak, while the latter report states that rendering a sintered sample into the form of a powder completely eliminates the extra-loss peak in $\chi_0''(T)$. Our data show that results appear to be a sensitive function of particle size and $|h^{ac}|$.

With a powder sample one has experimental complications due to a spread in the demagnetization factors of the particles, degree of particle isolation, i.e. filling factor, and problems with thermal gradients within the powder. Thus the absence of a discernable loss peak in $V_R(T)$ for the finely powdered sample, while interesting, must await further studies with carefully controlled particle sizes and filling factors before any meaningful conclusions may be drawn with regard to the effect which powdering a bulk sample has on its magnetic responses. Clearly the mere act of powdering the sample does not do away with the extra-loss peak.

The high ρ_n values of these oxides result in rather small values for $V_R(NS) \approx \Delta\chi_0''(NS)$ consequently its sign can be affected by incorrect phasing of the amplifier. Various checks made during the course of this investigation lead us to believe that the result, $\chi_0''(T \ll T_{co}) > \chi_0''(N)$ observed with some specimens is not an experimental artifact of the measuring technique per se. This is a disturbing result as it suggests that some regions of the sample are still in the mixed state at 77 K for rather modest values of h^{ac} . In the case of the melted sample data in the insert of Fig.4d clearly show that for $|h^{ac}| = 0.56$ Oe. the fully shielded state is only attained at $T \approx 55$ K.

4. χ_0^{ac} Frequency Effects

We conclude our discussion of the zero field ac magnetic susceptibility data with a few remarks concerning the effect of the ac measuring frequency for fixed $|h^{ac}|$. Taking the data for Nb, Fig.9, as being "typical" of an off-the-shelf superconductor one notes that the relative peak height, $\Delta V_R(PN)/\Delta V_R(NS)$, decreases with increasing frequency. This decrease in the relative height of the extra-loss peak with increasing frequency is associated with an increase in $\Delta V_R(NS) \approx \Delta\chi_0''(NS)$. It was this type of behavior for

superconducting elements and dilute alloys that led Maxwell and Strongin⁴² and others³¹ to develop eddy current models to explain the frequency dependence of the extra-loss peak in terms of normal state electrodynamics. According to these models there exists a critical frequency, f_c , above which the extra-loss peak will not be observed. Theory predicts that for a cylindrical sample of radius, a , $f_c = (1.8/a)^2 (10^9 \rho_n / 4\pi^2)$ with the normal state resistivity, ρ_n , in ohm-cm, a in cm, and f in sec^{-1} . It is this relationship between f_c and normal state electrodynamics has been challenged by the data of Couach et al²⁸. Cody and Miller⁵⁰ working with thin films of Pb observed the existence of an f_c and developed a modified eddy-current model which reproduced the above formula for f_c but one in which ρ_n is replaced with ρ_{ff} the flux flow resistivity. They used the measured f_c to calculate ρ_{ff} of their thin Pb films.

Assuming $\rho_n = 10^{-5}$ ohm-cm. for YBCO and $a = 0.2\text{cm.}$, the above expression yields a value of $\approx 10^4$ Hz for f_c . Goldfarb et al^{40,45} used a Nb sphere to calibrate their ac bridge and observed that the extra-loss peak in $\chi_0''(T)$ for sintered YBCO was invariant with frequency for $f=10, 100.$ and 1000Hz . Our data Fig. 10, is in qualitative agreement in the the extra-loss peak in $V_R(T)$ of the sintered sample is essentially undiminished at $f=950$ Hz. Higher frequency data on bulk samples is needed to shed light on the validity of the f_c predictions. Recently Worthington et al⁵¹ observed a large loss peak in 1 Mhz data on a single crystal of YBCO. Due to the smallness of the crystal, $a \approx 200$ μm a ρ_n of 10^{-5} ohm-cm. would require an f_c of order 10^7 Hz. It may be that Worthington et al⁵¹ have already disproved the normal state electrodynamical arguments if their 100 Mhz data showed an undiminished extra-loss peak in which case it would be useful to use the analysis of Cody and Miller⁵⁰ to calculate ρ_{ff} for their single crystal.

Increasing frequencies also have a curious effect on the $V_Q(T) \approx \Delta\chi_0'(T)$ data for the sintered sample. At 11 Hz one has a plateau which, with increasing values of f , becomes an inflection point at intermediate frequencies and is not discernable at the higher frequencies. In general an increase in f leads to a stronger attenuation of h^{ac} inside the sample. However in view of the relatively large ρ_n values one is hard put to attribute this effect to a decrease in δ_n as, at these frequencies, one expects $\delta_n >$ sample dimensions. Thus one is forced to speculate that some sort of relaxation effect in the SC of the grains per se. is responsible for this behavior. This of course leads to the question, why is this effect not seen in the melted samples? To study these frequency effects in any detail one needs a better designed cryostat than is available to us at this time as well as samples of controlled shape and surface conditions.

C. Magnetic field effects

Our interest in the effects of low dc magnetic fields centers around the reported reversible portion of the ZFC and FC magnetization data¹. If there is a portion of the magnetization curve which is thermodynamically reversible than one must observe a DPE³⁵. Traditionally measurements of the Meissner-Ochsenfeld effect have not been emphasized in studies of SC alloys and compounds for such systems do not display a Meissner effect²². Kittle in a recent comment⁵² discusses the prevalent appearances of Orymorons in scientific treatises, we would add to such a list the use of the term "partial Meissner effect". The Meissner effect relates to the exponentially decay of an applied dc magnetic field inside the SC region and requires that the magnetization curve be thermodynamically reversible. The phrase "a Meissner effect was observed" makes a definite statement with regard to the

thermodynamics of the NS transition. Partial flux expulsion, where the Meissner effect would yield "full" expulsion, provides little information about the thermodynamical reversibility of the magnetization curve or about the overall superconducting quality of the sample other than it is non-ideal from a thermodynamical point of view. If however one attributes the relatively smallness of the observed signal to a size effect^{4,11}, then the magnetic properties are still reversible and an appropriately scaled down DPE should be observed.

$T_{co}(H) = T_{co,H}$ is determined by the condition $|H - h^{ac}| = H_c(T_{co,H})$ or $H_{c2}(T_{co,H})$ and $T_{cc}(H) = T_{cc,H}$ is determined by the condition that $|H + h^{ac}| = (1-N)H_c(T_{cc,H})$ or $(1-N)H_{c1}(T_{cc,H})$. The former relation is a general one while the latter only applies to reversible magnetization curves showing a DPE. When hysteresis is present $T_{cc,H}$ is determined by the requirement that the amount of hysteresis is sufficiently large that the response to the ac field is one of perfect shielding³⁵. Thus one has the irony that a hysteretic superconductor can exhibit a sharper transition than a reversible one. If the magnetization curve is reversible for T near T_{co} then cooling the sample through T_{co} in the presence of an applied dc magnetic field, $H < (1-N)H_{c1}(T_1)$ where T_1 is spanned in the cooling procedure, must result in the observation of a DPE. We have examined the effects of applied fields of 5, 9, 11, 22, 38 Oe; values well below $H_{c1}(77\text{ K})$ and also in a field of 220 Oe. No evidence of a DPE was observed. Fig.5 presents selected traces to illustrate this point. The absence of a DPE³⁵ in the $V_Q(H,T) \approx \Delta\chi_H(T)$ traces, forces one to conclude that the "reversible" region of in the ZFC and FC scenarios is not a thermodynamically reversible one. Observed shifts in T_{co} in Fig.5a is surprising in that the initial slope of the upper critical field curve is so large

that no detectable shift was expected. While this is of secondary importance as far as the DPE is concerned, we are looking into this aspect of the data.

Besides the absence of a DPE the data, Figs.4 & 5, indicate that applied dc magnetic fields have a greater effect on sintered samples than on melted ones. Whereas a field of 220 Oe broadens considerably the $V_Q(H,T)$ trace of the sintered sample, midpoint displaced by -8 K, it has smaller effect on the corresponding trace of the melted sample. In this latter case the midpoint is only displaced by -1 K. One must note however that the transitions are incomplete at 77 K in agreement with the corresponding χ^{dc} data, Fig.3.

Data in Fig.5b show that the single, sharp loss peak observed in zero applied field for the sintered sample broadens with increasing H and develops structure. The main peak in $V_R(H,T) \approx \Delta\chi_H''(T)$ is displaced by -8 K in agreement with the shifts observed in the midpoints and inflections points of the $V_Q(T)$ traces. B. Barbara et al²⁹ have recently studied the extra-loss peak in some detail for single crystal and polycrystalline samples and find much substructure within a rather broad (≈ 25 K wide) "intragranular" peak for $|h^{ac}| = 2.0$ Oe. The observed dependence of T_p on $|h^{ac}|$ for values of h^{ac} between 0.1 and 45 Oe. was explained in terms of a nucleation model for supercurrent sheets across twin boundaries. We interpret their data as indicating a shift in T_p of about -10K when $|h^{ac}|$ is increased from small values to about 43 Oe. Clearly a 39 Oe dc field did not cause as large a shift in the high temperature peak in our samples. Thus large ac magnetic fields appear to have a more detrimental effect than do dc fields of comparable magnitude. Data for the melted sample, Fig 5d, show a much less dramatic effect in that the loss peak is only slightly broadened and no new structure appears in the $V_R(H,T)$ trace. Note that a dc field of 9 Oe destroys the substructure in the loss peak. An effect similar to what is observed with the

larger ac fields.

If we interpret the structure in the $V_Q(H,T)$ and $V_R(H,T)$ traces of Fig. 5a,b as being due to two distinct SC transitions and assign the higher temperature one to the grains per se and the lower temperature one to intergranular SC, we have a dilemma. Namely, if the sintered sample is composed of a system of weakly coupled grains why do we not observe similar traces for the partially melted samples. The micrographs, Figs. 1b indicate clusters of grains and the magnitude of the observed $V_Q(NS)$ requires the presence of macroscopic intragranular shielding currents of comparable magnitude to those responsible for the ac shielding of the sintered sample. This question draws attention to two facets of the sample's microstructure evident in the micrographs, Fig. 1b: (a) the clustering of grains of rectangular shapes and (b) the presence of a second, amorphous-like phase between clusters. Is the lack of any gross structure in the $V_Q(T)$ and $V_Q(H,T)$ transitions a result of the stronger pinning observed for these microstructures, is it a consequence of the shape and orientation of the crystallites or is it due to the second phase being present in the intercluster regions? These are open questions which are being explored at the present time.

V. Summary and Conclusions

The dc magnetization curves obtained at $T = 77$ K are typically those of a hysteretic, high κ superconductor. Recrystallization from the melt results in a material which exhibits a significantly increased hysteresis over that of the sintered material. Although there is no clear signature of granular behavior in these data, we have pursuant to common practice analyzed the magnetic hysteresis in terms of collection of isolated grains to arrive at values of

J_c (magnetic). Based on an average grain size as deduced from SEM we find that J_c (mag) for the melted sample is enhanced by a factor of 5 over that of the sintered sample. The observed decrease in J_c upon rendering the sample into the form of a fine powder suggests two possibilities: (1) the second phase present as intergranular material is playing a nonpassive role in the increased hysteresis which can only occur if intergranular currents are involved in the magnetic hysteresis or (2) the enhanced hysteresis in the bulk may be the result of a fortuitous alignment of the crystallites or cluster of grains which is destroyed by the act of powdering the sample. After this work was completed we learned of a similar study by Jin et al⁵³ who found a similar increase in magnetic hysteresis but a smaller increase, i.e. a factor of two, in J_c (mag) due to an increase in the average size of the grains in the recrystallized from the melt sample. No data were reported on the effects of powdering or on the ac responses of their material. Based on a survey of the literature the dc magnetic properties of these high T_c oxides are generally reproducible among the numerous laboratories involved in this area of research. One can not make a similar statement with regard to reports concerning the responses of these materials to ac magnetic fields.

Although ac inductance techniques have been used in the search for, and study of, superconductors for at least fifty years there is a disturbing amount of inconsistencies in the interpretation of such data. Whereas the previous misconception between "perfect ac shielding" and the Meissner Ochsenfeld effect in measurements of $\Delta\chi_0''$ (NS) is now generally recognized, recent problems have arisen with regard to the significance of the "extra-loss peak" in measurements of $\Delta\chi_0''$ (NS). The large disparity in reported χ_0'' (T) data as regards the number and magnitude, of the extra-loss peaks as well the significance of substructure with a given peak, is a cause for concern.

One may simply dismiss this as "experimental artifacts" due to incorrect techniques or be confounded by the apparent myriad of ac responses which different processing techniques of this multicomponent system can produce. Equally disturbing are the vicissitude of responses found within a given processing technique. For example how can a sintered specimen show the double transition ala Raboutou et al⁴¹ and not be evident in the numerous reported measurements of $\chi_0'(NS)$. Another one is the effect of powdering which varies from no effect on, to a complete absence of, the extra-loss peak which occurs in $\chi_0''(T)$ of sintered samples. While one may account for differences in the detailed behavior of $\chi_0''(T)$ to differences in experimental techniques, gross variations in qualitative responses seem to require a different explanation. We are inclined to believe that surface effects are responsible for the latter state of affairs as surface effects should be more evident in ac measurements than in dc measurements

A straightforward application of the inter- vs intrashielding concepts to our $\Delta\chi_0'(T)$ and $\Delta\chi_0''(T)$ data poses a dilemma. For the sintered sample at low values of h^{ac} and f , one has evidence for two transitions in the $V_Q(T) \approx \Delta\chi_0'(T)$ traces yet only a single loss peak is observed in $V_R(T) \approx \Delta\chi_0''(T)$. The correlation of the loss peak with the inflection in the $V_Q(T)$ trace along with the observed R_{dc} vs T transition requires one to postulate that intergranular shielding becomes dominant at a temperature very close to T_{c0} and that any loss peak associated with the grains per se is small and/or masked by the steep onset of the intergranular shielding. Increasing the value of $|h^{ac}|$ at fixed frequency shifts the loss peak to lower temperatures and produces substructure in the loss peak. In the case of the melted sample just the opposite effect is noted. Thus the effect of essentially allowing the ac field to "probe" more deeply into the sample produces a variety of effects.

Increasing the ac measuring frequency at fixed h^{ac} which causes the ac field to "probe" less deeply into the sample, has no major effect on the ac responses but seems to enhance the double transition apparent in the $V_Q(T)$ data for the sintered sample. The persistence of a sizable loss peak at frequencies approaching 10^3 Hz confirms in a contactless measurement, via eddy current models, that these materials are high ρ_n materials in comparison to d-electron superconductors such as Nb.

Since the pioneering work of Hudson⁵⁴, powdering a sample has been used to eliminate the ac shielding affects associated with the presence of a superconducting network due to a minority phase in measurements of $\chi_0'(T)$. Present efforts with the oxides focus on the effect which powdering has on the appearance and shape of the extra-loss peak in measurements of $\chi_0''(T)$. While we have not studied this aspect in any detail, data of Fig.6 suggest that here one must be concerned with a size effect. In any discussion of these high T_c oxides the role of crystalline anisotropy is always of concern. Anisotropy could, in principle, smear out any small loss peak associated with differently orientated grains but should have no effect on the intergranular losses associated with clustering of the grains in course powders.

The presence of an externally applied dc magnetic field clearly has a much stronger effect upon the ac responses of the sintered samples than upon those of the melted samples. This is in contrast to the χ^{dc} data which show comparable behavior for the two samples. Thus the χ^{ac} data show the effects of increase pinning in a more dramatic fashion than do the χ^{dc} data. Based on the $\Delta\chi_H''(T)$ results one is inclined to say that a variety of pinning mechanisms are operative in the sintered material while one pinning mechanism seems to be dominant in the melted material. Microstructures of the melted samples consists of randomly oriented clusters of rectangularly

shaped grains separated by an amorphous-like second phase. At the present time we can not state whether the increased pinning, also in evidence in the magnetization curves, is due to the grains per se or due to the second phase. Although the effect observed upon powdering the sample is suggestive of a non passive role for the second phase, we feel the results are ambiguous due to experimental limitations previously discussed.

The present study leads to two general conclusions. The first is that a direct comparison of magnetization curves and ac magnetic susceptibility data of sintered, and recrystallized from the melt, samples show that the latter samples are strong pinning materials at 77 K. Thus recrystallization from the melt is a viable route to produce coarse powders of enhanced SC properties for the fabrication of thick SC films of potential importance in emerging technologies. Ways to allieviate the relatively large ac losses at very modest field levels at 77 K must be found before the full technological potential of these materials can be exploited.

The other conclusion is a more general one and is that nonstoichiometry and associated lack of crystallographic long range order leading to surface effects should be considered as possible causes of the considerable differences that exist in reported $\chi_0''(T)$ data. Although a direct comparison of published data is hindered by the manner in we experimentalist report our data, there are simply too many qualitative inconsistencies to be attributed solely to grain boundry effects and intergranular superconductivity.

VII REFERENCES

1. G. W. Crabtree, W. K. Kwok and A. Umezawa "Basic Properties of Oxide Superconductors" in Quantum Field Theory as an Interdisciplinary Basis, F. C. Khanna, H. Umezawa, G. Kunstatter and H. C. Lee, eds. World Scientific Publ. Co. Ltd. 1988. J. Muller, "Materials Elaboration and Electronic Properties of High T_c Oxide Superconductors", Proc. of Genova Conference, July 1-3, 1987.
2. There are numerous reviews on this subject. Two typical reviews are: A. P. Malozemoff, W. J. Gallagher and R. E. Schwall, Amer. Chem. Soc. Sym. Sept 1987 and M. Nissenoff, Cryogenics Jan. (1988).
3. J. R. Clem and V. G. Kogan, Jpn. J. A. P., 26, 1161 (1988), Suppl. 26-3..
4. D. K. Finnemore, R. N. Shelton, J.R. Clem, R. W. McCallum, H. C. Ku, R. E. McCarley, S. C. Chen, P. Klavins, V. Kogan, Phys. Rev. B35, 5319 (1987).
5. A. Benziger, J. L. Jorda and J. Muller, S. S. Comm. 1987).
6. A. Junod, A. Bezing T. Graf, J.L. Jorda et. al. , Europhys. Lett. 4, 247 (1987). see also A. Junod, A. Bezing and J. Muller, Physica C 52,?? (1988).
7. W. Meissner and R. Ochsenfeld, Naturwissenschaften 21, 787 (1933).
see any elementary solid state physics text book.
8. The acronyms FC and ZFC are commonplace in recent publications: e. g. see J. R. Thompson, D. K. Christen, S. T. Sekula, J. Brynestad and Y. C. Kim, J. Mater. Res. 2, 779 (1987). and D. C. Cronmeyer, A. P. Malozemoff and T. R. McGuire, Mat. Res. Symp. Proc. 99, 837 (1988).
9. D. S. Ginley, E. L. Venturini, J. F. Kwak, R. J. Baughman, B. Morosin and J. E. Schirber, Phys. Rev. B 36, 829 (1988).
10. N. Garcia, S. Vieira, A. M. Baro et al., Z. Phys. B 70, 9 (1988).

11. D. E. F. Farrell, M. R. DeGuire, B. S. Chandrasekhar, S. A. Alterovitz, P. R. Aron, and R. L. Fagaly, Phys. Rev. B 35, 8797 (1987). Also see M. R. De Guire and D. E. Farrell, Adv. Cerm. Maters. 2, No.3B 593 (1988).
12. H. Hojaji, K. A. Michael, A. Barkett, A. N. Thrope, M. Ware, I. Talmy, D. Haught and S. Alterescu, J. Mater. Res. to appear.
13. H. Hojaji, A. Barkatt, and R. A. Hein, Mat. Res. Bull. 23, 869 (1988).
14. A. N. Thrope and F. E. Senftle, Rev. Sci. Instrum. 30, 1006 (1959).
15. E. Maxwell, Rev. Sci. Instrum. 36, 533 (1965).
16. J. Z. Sun, D. J. Webb, M. Naito, K. Char, M. H. Hahn, J. W. P. Hsu, A. D. Kent, D. B. Mitzi, B. Oh, M. R. Beasley, T. H. Geballe, R. H. Hammond, and A. Kapitulnik, Phys. Rev. Lett. 58, 1574 (1987); A. Umezawa, G. W. Crabtree, J. Z. Liu, H. W. Weber, W. K. Kwok, L. H. Nunez, T. J. Moran, C. H. Sowers and H. Claus, Phys. Rev. B36, 7151 (1987); E. McHenry J. McKittrich, S. Sasayama, V. Kwapong, R. C. O'Handley and K. G. Kalonji, Phys. Rev. B 37, 623 (1988).
17. G. Xiao, F.H. Streitz, A. Gavrin, M. Z. Cieplak, J. Childress, M. Lu, A. Zwicker and C. L. Chien, Phys. Rev. B36, 2382 (1987) and Ref.16.
18. D. G. Schweitzer and B. Bertman, Phys. Rev. 152, 293 (1966). 19. W. A. Fietz and W. W. Webb, Phys. Rev. 178, 657 (1969).
20. C. P. Bean, Phys. Rev. Lett. 8, 250 (1962). 21. J. R. Thompson, D. K. Christen, S. T. Sekula, J. Brynstad and Y. C. Kim, J. Mater. Res. 2, 779 (1987).
21. J. R. Thompson, D. K. Christen, S. T. Sekula, J. Brynstad and Y. C. Kim, J. Mater. Res. 2, 779 (1987).
22. D. Shoenberg, Superconductivity, Cambridge University Press, London, U. K., 1965, p. 1202.
23. J. R. Clem, H. R. Kerchner and S. T. Sekula, Phys. Rev. B14, 1893 (1976).

24. A early example is found in B. Renker, I. Apfelstedt, H. Kupfer, C. Politis, H. Rietschel, W. Schauer, H. Wuhl, U. Gottwick, H. Kniessel, U. Rauchschalbe, H. Spille and F. Steglich, Jpn. J. A. P. 26 1169 (1987). Suppl.26-3.
25. E. Polturak and B. Fisher, Phys. Rev. B36, 5586 (1987).
26. E. Laurmann and D. Shoenberg, Proc. Roy. Soc. Lond. A198 560 (1949).
27. A. F. Khoder, Phys. Lett. 8, 378 (1983).
28. M. Couach, A. F. Khoder and B. Barbara, Cryogenics 25 695 (1985).
This paper presents a fine review of the ac inductance technique and presents some intriguing data in support of Khoder's theory.
29. B. Barbara, A. F. Khoder, M. Couach, and J. Y. Henry, Europhys. Lett. 6, 612 (1988).
30. B. T. Matthias, T. H. Geballe, R. H. Williams, E. Corezvit, and G. W. Hull, Jr., Phys. Rev. 139 A1501 (1965).
31. R. A. Hein, Phys. Rev., B33, 7539 (1986).
32. C. Kittle, S. Fahy and S. G. Louie, Phys. Rev. B37, 642 (1988).
33. K. Mendelssohn, Proc. Roy. Soc. A152, 34 (1935).
34. For a general review see "Inhomogeneous Superconductors" AIP proceedings #58. D.U. Gubser and S. A. Wolf Eds. (1978).
35. R. A. Hein and R. L. Falge, Jr., Phys. Rev. 123, 407 (1961).
36. In calculating a ΔT_c for the higher $|hac|$ values we have taken for the melted samples $V_Q(77\text{ K}) \approx 0.9 V_Q(S)$. Based on data obtained down to 4.2 K (insert of Figure 3b) this estimate should be good to a few percent.
37. B. N. Das, J.E. Cox, R.W. Huber and R.A. Meussner, Metall. Trans., 8A 541 (1977). See also Ref. 28 for similar results with V_3Si .
38. M. Osofsky, S. A. Wolf, L. E. Toth and R. A. Hein, unpublished results.

39. A. Junod, A. Bezing, D. Cattani, J. Cors, M. Decroux, O. Fischer, P. Genoud, L. Hoffmann, J. L. Jorda, J. Muller, and E. Walker, Jpn. J. A. P. 26 1021 (1987), Suppl. 26-3.
40. R. B. Goldfarb, A. F. Clark, A. I. Braginski and A. J. Panson, Cryogenics, 27 475 (1987).
41. A. Raboutou, P. Peyral, J. Rosenblatt, C. Lebau, O. Pena, A. Perrin, C. Perrin and M. Sergent, Euophys. Lett. 4 1321 (1987).
42. E. Maxwell and M. Strongin, Phys. Rev. Lett. 10 212 (1963).
43. There are several variations in the mathematics used in the development of this model, e.g. C. A. M. van der Klein, J. D. Elen, R. Worf, and D. de Klerk, Physica 49 98 (1970). R. W. Rollins and J. Silcox, Phys. Rev. 155 404 (1967).
44. T. Ishida and H. Mazaki, Jpn. J. Appl. Phys. 52 6793 (1981).
45. R. B. Goldfarb, A. F. Clark, A. J. Panson and A. I. Braginsky, Materials Research Soc., Anaheim Calif. (1987).
46. C. Ayache, B. Barbara, E. Bonjour, P. Burlet, R. Calemczuk, M. Couach, M. J. G. M. Jurgens, J. Y. Henry and J. Rossat-Mignod, Physica, B148 305 (1987).
47. B. Renker, I. Apfelstedt, H. Kupfer C. Politis, H. Rietschel, W. Schauer, and H. Wuhl, Z. Phys. B67 1 (1987).
48. H. Kupfer, S. M. Green, C. Jiang, Yu Mei, H. L. Luo, R. Meier-Hirmer and C. Politis, Z. Phys. B71 63 (1988).
49. I. Apfelstedt, R. Flukiger, H. Kupfer, R. Meier-Hirmer, B. Obst, C. Politis, W. Schauer, F. Weiss, and H. Wuhl, Jpn. J. A. P., 26 1181. (1987) Suppl.26-3.
50. G. D. Cody and R. E. Miller, Phys. Rev. 173 481 (1968).
51. T. K. Worthington, W. J. Gallagher, D. L. Kaiser, F. H. Holtzberg and T. R.

- Dinger, Physica C153-155, 32 (1988).
52. C. Kittle, Phys. Today, p.93, May (1988).
53. S. Jin, R. C. Sherwood, E. M. Gyorgy, T.H. Tiefel, R. B. van Dover, S. Nakahara, L. F. Schneemeyer, R. A. Fastnacht, and M. E. Davis, Appl. Phys. Lett. 54, (1988).
54. R. P. Hudson, Phys. Rev. 29, 283 (1950).
- xx R. W. McCallum, W. A. Karlsback, T. R. Radhakrishnam, F. Pobell, R. N. Shelton and P. Klavins, Solid. State Commun. 42, 819 (1982).
- xx. H. A. Ullmaier, phys.Stat. Sol. 17, 631 (1966).
- 51.

VII, FIGURE CAPTIONS

1. Scanning electron micrographs of superconducting $\text{YBa}_2\text{Cu}_3\text{O}_x$ specimens: (a) sintered (990°C), 2000 x magnification; (b) recrystallized-from-the-melt (1050°C), 500 x magnification..
2. Magnetic moment as a function of applied dc magnetic field at $T = 77\text{ K}$: (a) sintered specimen and (b) recrystallized-from-the-melt specimen. Inserts show $J_c(H, 77\text{ K})$ deduced from the magnetization curves
3. DC magnetic susceptibility as a function of temperature for three values of the applied magnetic field: (a) sintered specimen and (b) recrystallized-from-the-melt specimen
4. (a) Imbalanced voltage $V_Q^*(T) \approx \Delta\chi_0'(T)$ of the sintered specimen as a function of temperature for $|h^{ac}| = 0.13, 0.51, 0.91, 1.5, 3.1$, and 6.3 Oe . Curves 1 - 6 respectively. $V_Q^*(T) = (V_Q/T)/h^{ac}(0.091)$ for a amplifier gain of 10^3 . (b) $V_R(T) \approx \Delta\chi_0''(T)$ as a function of temperature for the same values of $|h^{ac}|$. (c) $V_Q^*(T)$ and (d) $V_R(T)$ for the melted specimen for $|h^{ac}| = 0.09, 0.23, 0.91$, and 9.1 Oe . Curves 1-4 respectively. (e) $V_Q^*(T)$ and (f) $V_R(T)$ for a melted specimen as a function of temperature for $f = 17\text{ Hz}$ and $|h^{ac}| = 0.028, 0.12, 0.57$ and 1.1 Oe .; curves 1-4 respectively.
5. (a), (b) Imbalanced voltages $V_Q(T)$ and $V_R(T)$ for the sintered specimen as a function of temperature for $H = 0, 0.89, 18, 37, 120$ and 220 Oe .; curves 1-6 respectively. (c), (d) similar data for the melted specimen.
6. Imbalanced voltages $V_Q(T)$ and $V_R(T)$ as a function of temperature for two powdered specimens: (a) 560 mg coarse powder, $h^{ac} = 0.57\text{ Oe}$; (b) 180 mg of the fine powder, $h^{ac} = 0.76\text{ Oe}$. Inserts

show the dc magnetization and susceptibility data for the finely powdered specimen.

7. R_{dc} and simultaneously obtained $V_Q(T)$ and $V_R(T)$ as functions of temperature for sintered YBCO. (NRL unpublished).
8. $\Delta M'(T)$ and $\Delta M''(T)$ for a $TiCr_{1.65}$ alloy specimen as functions of temperature for $|h^{ac}| = 0.002, 0.05, 0.20$ and 1.00 Oe.; curves 1-4 respectively (J. W. Gibson and R. A. Hein unpublished).
9. (a) $\Delta M'(T)$ and $\Delta M''(T)$ for an annealed Sn specimen as a function of temperature (JWG/RAH unpublished); (b), (c) $V_Q(T)$ and $V_R(T)$ for a machined cylinder of Nb as a function of temperature for two values of the ac measuring frequency.
10. Imbalanced Voltages $V_Q(T)$ and $V_R(T)$ with $|h^{ac}| = 0.12$ Oe for several values of the ac measuring frequency. $f = 11, 44, 110$, and 440 Hz, curves a-d respectively. Note shifts in the zeros of the y-axis and overall amplifier gains.

- ? $\Delta M''(T)$ and $\Delta M'(T)$ of $TiCr_{1.65}$ as a function of temperature for several values of applied dc magnetic field. (JWG/RAH unpublished).
- ? Imbalanced voltages $V_Q(T)$ and $V_R(T)$ as a function of temperature for several values of the ac measuring frequency with $|h^{ac}| = 0.13$ Oe.

ORIGINAL PAGE IS
OF POOR QUALITY



(a)



(b)

Figure 2a

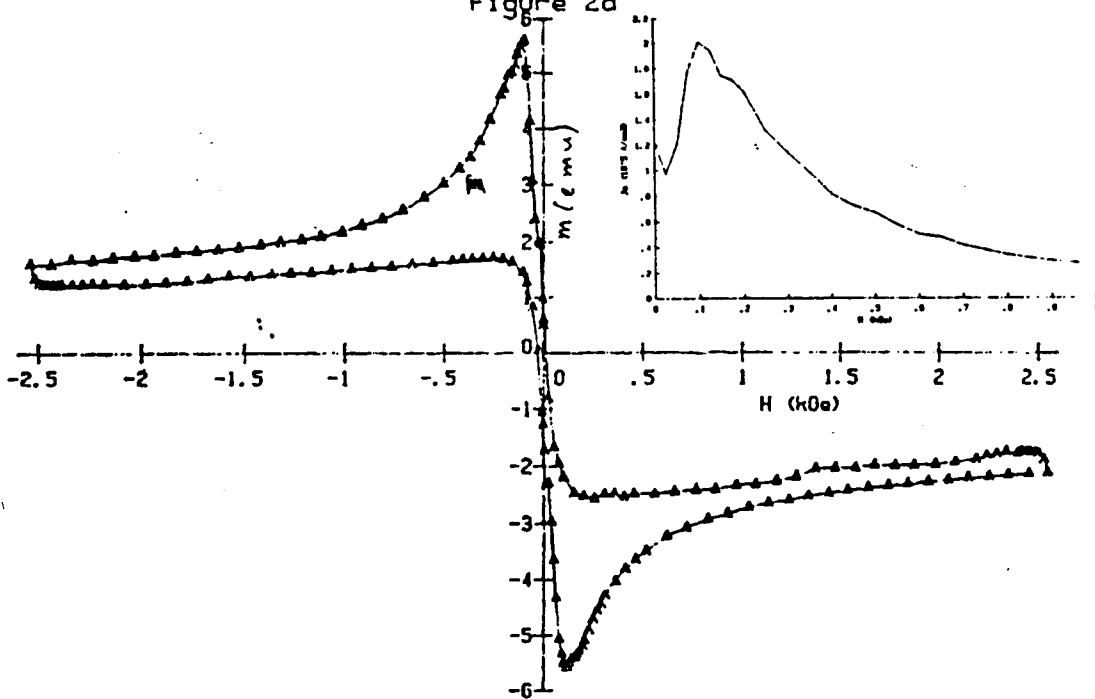


Figure 2b

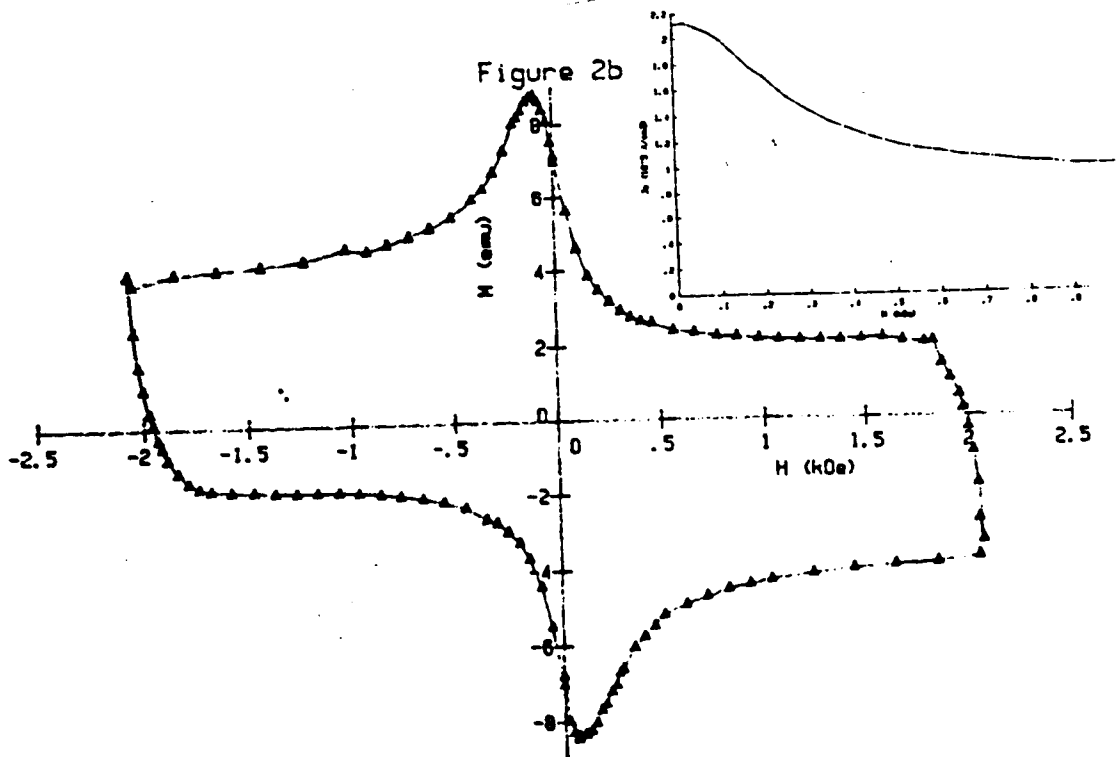


Figure 3a

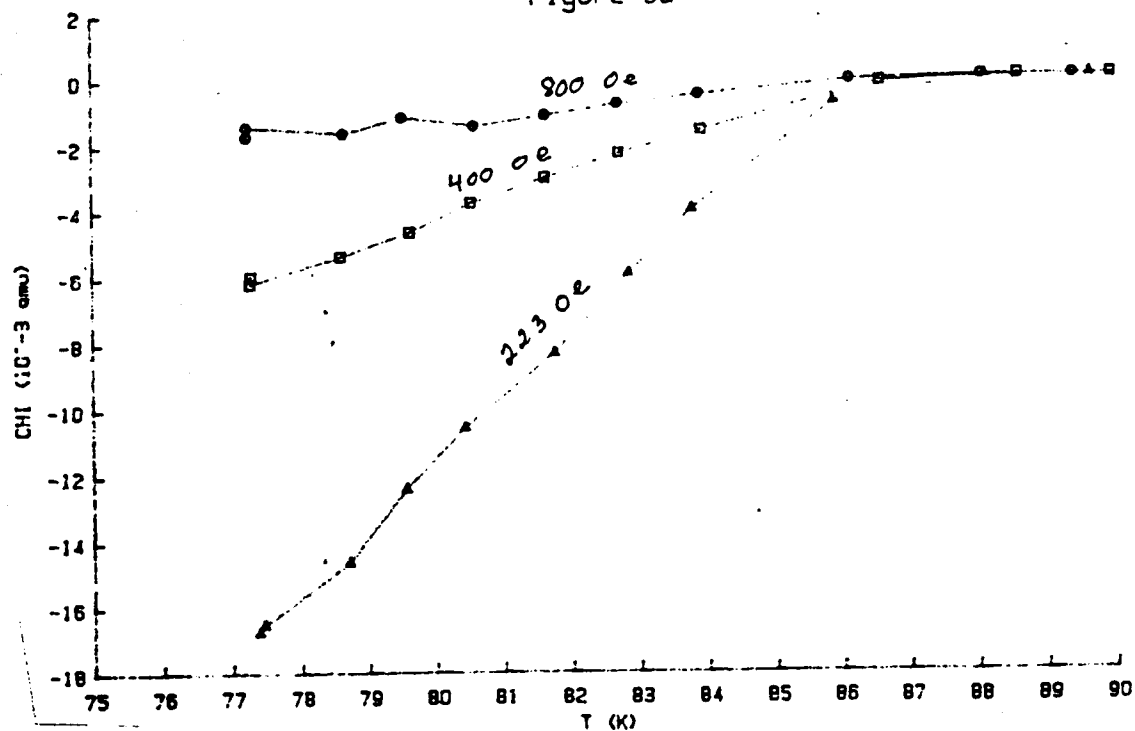
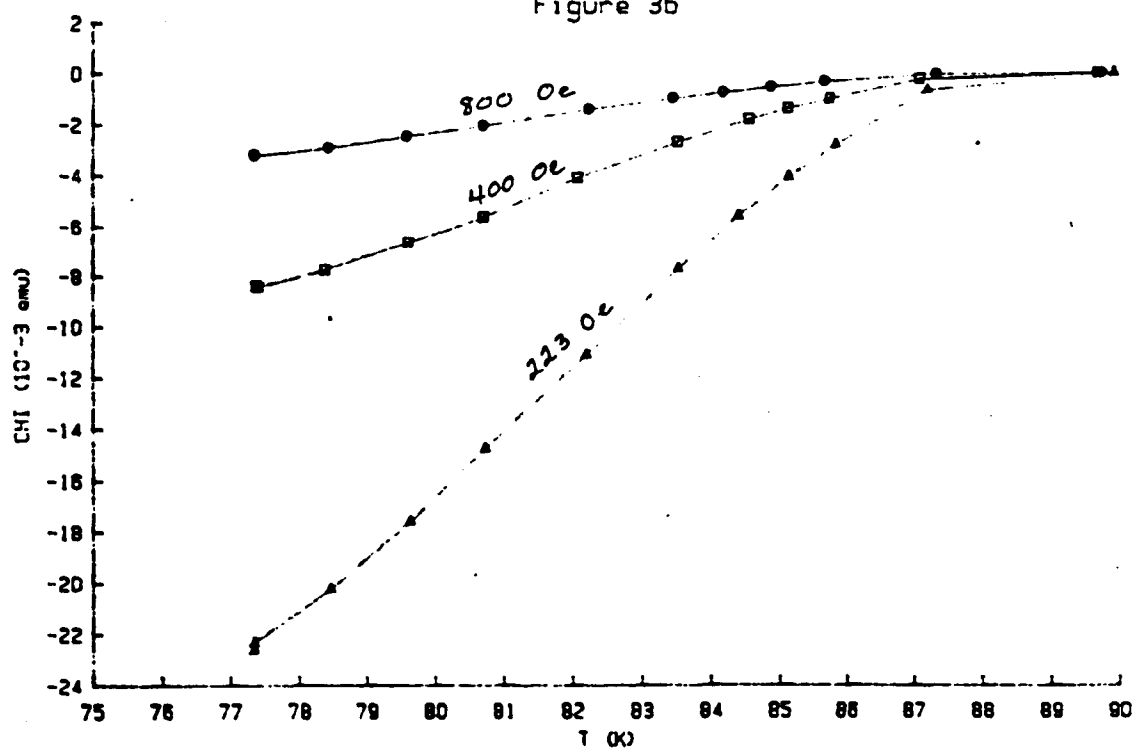


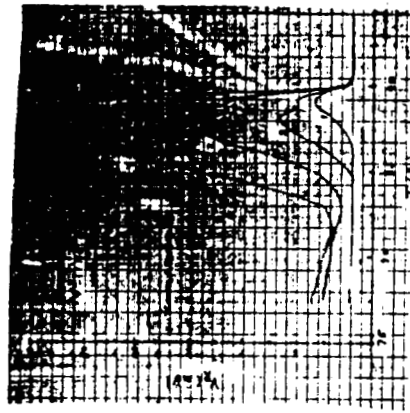
Figure 3b



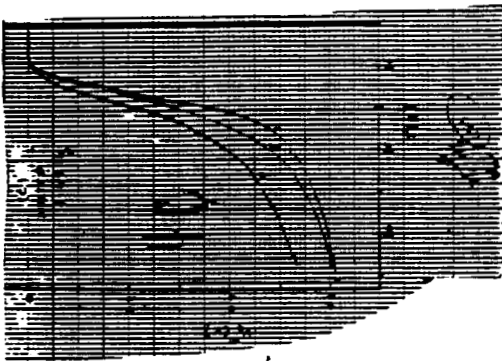
ORIGINAL PAGE IS
OF POOR QUALITY



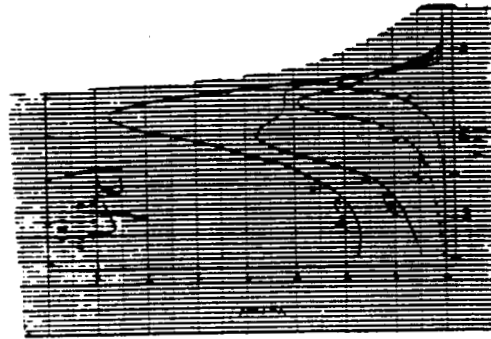
4e



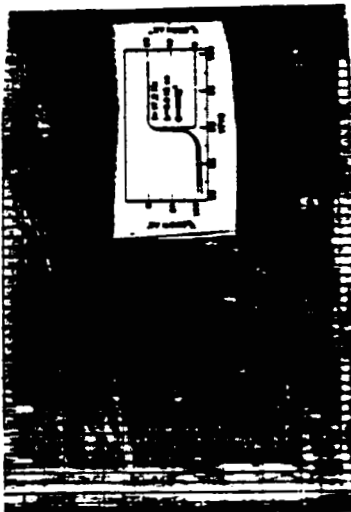
4f



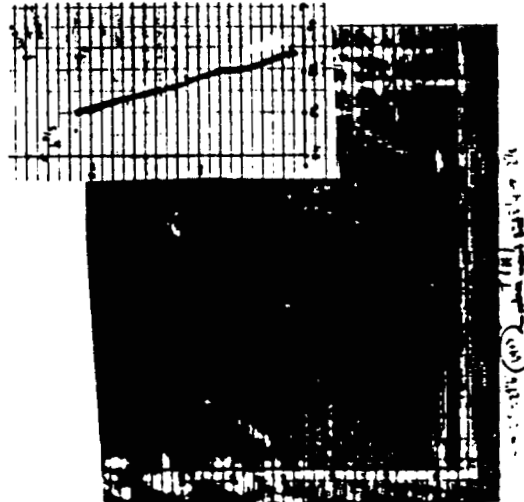
4c



4d



4a



4b

ORIGINAL PAGE IS
OF POOR QUALITY

